TECHNO-ECONOMIC AND THERMODYNAMIC OPTIMIZATION OF LOW-TEMPERATURE RANKINE CYCLES

Inés Encabo-Cáceres[*], Roberto Agromayor, Lars O. Nord

Department of Energy and Process Engineering, Norwegian University of Science and Technology (NTNU)

Trondheim, Norway

[*]iencaboc@gmail.com

ABSTRACT

This paper covers the thermodynamic and techno-economic optimization of ORCs for low-to-medium temperature heat source applications, when ammonia, propylene, R152a and R32 are used as cycle working fluids. Results were obtained for a varying hot source inlet temperature, from 120°C to 250°C, and different capacity power plants, showing that the most efficient ORC power plants always had a higher Specific Investment Costs (SIC) for the studied cases. Large-capacity power plant (power output between 1 and 2.5 MW) are more expensive than the small-capacity ones (power output below 1 MW) but the SIC of large-capacity systems can be half of that of small-capacity systems. Minimizing the SIC of ORCs tends to higher evaporating and condensing temperatures than the ones that result from the thermodynamic optimization.

Keywords: Organic Rankine Cycle, heat exchanger, shell and tube, plates, second law, exergy, efficiency

NONMENCLATURE

Abbreviations	
calc	Calculated
c	Cold fluid
cond	Condenser
h	Hot fluid
f	Working fluid
LCOE	Levelized Cost of Electricity
LMTD	Logarithm Mean Temperature Difference
ORC	Organic Rankine Cycle
pp	Pinch point
PrHE	Primary Heat Exchanger
sat	Saturated
SQP	Sequential Quadratic Programming
SIC	Specific Investment Cost
sc	Subcooling
sh	Superheating
f	Working fluid

Symbols		
A	[m^2]	Area
C_P	[$]	Basic Cost
CF	[m^2] or [kW]	Capacity Factor
C	[$]	Cost
d	[m]	Diameter
η	[-]	Efficiency
h	[kJ/kgs]	Enthalpy
$\dot{E}$	[kW]	Exergy flow rate
$\dot{Q}$	[W]	Heat power
U	[W/m^2·K]	Heat transfer Coefficient
$\dot{m}$	[kg/s]	Mass flow rate
$\dot{W}$	[kW]	Power
p	[Pa]	Pressure
η_{II}	[-]	Second law efficiency
d_s	[m]	Shell diameter
T	[K] or [°C]	Temperature

1. INTRODUCTION

During the last years, ORC technology has grown in the market and big efforts are being put into its development. Applications include low-temperature geothermal energy, waste heat recovery from industry, and many other where conventional water-based Rankine cycles or gas-based Brayton cycles are not the best solution. Most authors agree that thermodynamic optimization alone is not a definitive indicator for determining the most suitable ORC configuration, mainly because each working fluid and each thermodynamic parameter has a great impact not only on the efficiency of the cycle, but also on its cost. Quoilin et al. completed both optimizations in [2], without taking into consideration the fluid properties in the thermodynamic analysis, and they found that the economics profitability and the thermodynamic efficiency lead to different optimal working conditions.

Le et al. concludes the same in [3]: the configuration that leads to the ORC maximum exergy efficiency is not the most profitable one. Their analysis used LCOE as the

economic objective function, and it included pressure losses and heat transfer coefficients in the calculations. Other authors, such as Imran et al. [4], presented a multi-objective optimization, in which they combined both the thermodynamic and the techno-economic optimization, considering different ORC layouts. Results show that increasing the evaporation and condensation temperatures leads to better efficiencies and lower costs, and that high degrees of superheating normally yield better efficiencies but higher costs. Kazemi et al. optimized the second law efficiency and SIC of a new proposed ORC in [5]. Results show that, even though this new configuration may present higher efficiencies than the simple ORC, its optimum SIC is normally higher. Therefore, most authors agree that increasing ORCs' efficiency requires higher investments.

Even though many authors have focused their studies on the thermodynamic and techno-economic optimization of ORCs, there is still a lack of information regarding which parameters are the most important for the optimization of the system. Each author sets different degrees of freedom, and most of them agree on the impact that the condensing and evaporating temperatures have on the results. However, even though authors agree that heat exchangers cost represents a great share of the total cost, and that their design may determine the ORC efficiency, most of them assume fixed values for all geometry design variables. In order to fill this gap, this work is focused on the thermodynamic and techno-economic optimization of ORCs, setting the fluid properties and heat exchanger parameters that have an impact on the performance and cost of the cycle as degrees of freedom.

2. METHODOLOGY

2.1 Rankine cycle model

A steady-state model for subcritical Rankine cycles was developed and implemented in MATLAB. The model assumes constant isentropic efficiencies for turbine and pump and it uses the first law of thermodynamics and the REFPROP fluid library to compute all the cycle states in a sequential way.

A plates heat exchanger was adopted for the condenser whereas a shell-and-tube heat exchanger was chosen for the primary heat exchanger, due to the pressure and temperature limitations of plates heat exchangers [6]. The heat exchangers were discretized in $N = 25$ elements to locate the pinch point and to use suitable heat transfer and pressure drop correlations depending on the state of the working fluid. The heat transfer and pressure drop correlations used in this work are reported in detail in [7].

Once the heat transfer coefficient associated with each node is determined, the heat transfer area of each discretization is computed using the Logarithmic Mean Temperature Difference (LMTD) method. The total area of the heat exchanger is determined summing the area of every discretization:

$$A = \sum_{i=1}^{N} A_i = \sum_{i=1}^{N} \left(\frac{\Delta T_{\mathrm{LMTD}}}{U \cdot \dot{Q}} \right)_i \qquad (1)$$

The cost of the system was estimated using the correlations proposed by Turton [8] because it has been used in the past by several authors to analyze the cost of low-temperature Rankine cycles [5, 9, 10, 11]. The main formula proposed by Turton is given by:

$$\log C_P = K_1 + K_2 \log_{10}(CF) + K_3 (\log_{10}(CF))^2 \qquad (2)$$

Where the formulas used to obtain C_P, K_i and CF are described in detail in the original publication [7].

2.2 Optimization problem formulation

In order to optimize the performance of the Rankine cycle, it is necessary to specify the objective function to be optimized, the values of the fixed parameters, the independent variables and the constraints that limit the design space. In this work, the performance of the Rankine cycle was optimized with respect to two objective functions:

- *For the thermodynamic optimization*, the second law efficiency was used because it gives insight about how much potential for improvement is left [12, 13].

$$\eta_{II} = \eta_{\mathrm{II,cycle}} \cdot \eta_{\mathrm{recovery}} = \frac{\dot{W}_{\mathrm{net}}}{\dot{E}_{\mathrm{in}}} \cdot \frac{\dot{E}_{\mathrm{in}}}{\dot{E}_{\mathrm{max}}} = \frac{\dot{W}_{\mathrm{net}}}{\dot{E}_{\mathrm{max}}} \qquad (3)$$

- *For the techno-economic optimization*, the SIC was set as objective function to find a solution that tries to maximize power output and minimize cost.

$$SIC = \frac{C_{\mathrm{total}}}{\dot{W}_{\mathrm{net}}} \qquad (4)$$

The fixed parameters, independent variables and inequality constraints used in this work are summarized in *Table 1*. In addition, four equality constraints are used to ensure that the pressure drops at each side of the heat exchangers specified as degrees of freedom are consistent with the pressure drops computed from the pressure drop correlations. A sequential quadratic programming algorithm (SQP) was used to solve the optimization problem.

2

Results are reported for ammonia, propylene, R32 and R152. These fluids where selected based on the results from a previous work by the authors [7].

Table 1: Optimization problem formulation

Fixed parameters		
Heat source		
$\dot{m}_{\mathrm{h}}$	[kg/s]	10
$T_{\mathrm{h,\,in}}$	[°C]	120
$p_{\mathrm{h,\,out}}$	[bar]	3
Heat sink		
$T_{\mathrm{c,\,in}}$	[°C]	10
$p_{\mathrm{c,\,in}}$	[bar]	1
Turbomachinery efficiency		
η_{pump}	[%]	70
η_{turbine}	[%]	80
Shell and tube heat exchanger (primary heat exchanger)		
Pitch layout		Triangle
N_{p} and N_{s} No. of passes and shells	[-]	1
L_{b} Baffle length	[-]	$0.25 \cdot d_{\mathrm{s}}$
B Baffle spacing	[-]	$0.50 \cdot d_{\mathrm{s}}$
Plates heat exchanger (condenser)		
β Chevron angle	[°]	45
b Corrugation height	[mm]	2
N_{p} Number of passes	[-]	1
t Plate thickness	[mm]	5

Independent variables			
$T_{\mathrm{h,\,out}}$	[°C]	[15	85]
$\Delta T_{\mathrm{c,\,cond}}$	[°C]	[2	10]
$p_{\mathrm{turbine,\,in}}$	[bar]	$[p_{min}$	$0.9\,p_{\mathrm{crit}}]$
$p_{\mathrm{turbine,\,out}}$	[bar]	$[p_{min}$	$0.9\,p_{\mathrm{crit}}]$
$h_{\mathrm{turbine,\,in}}$	[kJ/kgs]	$[h_{\min}$	$h_{max}]$
$h_{\mathrm{PrHE,\,in}}$	[kJ/kgs]	$[h_{\min}$	$h_{\max}]$
$\Delta p_{\mathrm{h,\,PrHE}}$	[-]	[0.1%	15%]
$\Delta p_{\mathrm{f,\,PrHE}}$	[-]	[0.1%	20%]
$\Delta p_{\mathrm{f,\,cond}}$	[-]	[0.1%	15%]
$\Delta p_{\mathrm{c,\,cond}}$	[-]	[0.1%	-]
Shell and tube heat exchanger (primary heat exchanger)			
d_{o} Tubes outlet diameter	[mm]	[35	510]
t Wall thickness	[mm]	[3	15]
v_{f} Tubes working fluid velocity	[m/s]	[0.9	2.6]
$d_{\mathrm{o}}/d_{\mathrm{i}}$ Pitch to outer diameter ratio	[-]	[1.25	1.50]
Planes heat exchanger (condenser)			
V_{ch} Volume flow per channel	[m³/h]	[0.50	12.50]
L_{h} Plate width	[m]	[0.50	3.25]

Nonlinear constraints			
$\Delta T_{\mathrm{f,\,sc}}$	Degree of subcooling	[°C]	≥ 0
$\Delta T_{\mathrm{f,\,sh}}$	Degree of superheating	[°C]	≥ 0
$\Delta T_{\mathrm{PrHe,\,pp}}$	Pinch point temp. diff.	[°C]	≥ 5
$\Delta T_{\mathrm{cond,\,pp}}$	Pinch point temp. diff.	[°C]	≥ 5
SIC	Specific Investment Cost	[$/kW]	≥ 0

$\Delta p_{\mathrm{h,\,PrHE,calc}}$	Calc. hot PrHE pres. drop	[-]	$= \Delta p_{\mathrm{h,\,PrHE}}$
$\Delta p_{\mathrm{f,\,PrHE,calc}}$	Calc. fluid PrHE pres. drop	[-]	$= \Delta p_{\mathrm{f,\,PrHE}}$
$\Delta p_{\mathrm{f,\,cond,calc}}$	Calc. fluid cond. pres. drop	[-]	$= \Delta p_{\mathrm{f,\,cond}}$
$\Delta p_{\mathrm{c,\,cond,calc}}$	Calc. cold cond. pres. drop	[-]	$= \Delta p_{\mathrm{c,cond}}$

Observations:

$$p_{\min} = p_{\mathrm{sat}}(T_{\mathrm{c,\,in}})$$
$$h_{\min} = h_{\mathrm{sat}}(T_{\mathrm{c,\,in}})$$
$$h_{\max} = h(T_{\mathrm{h,\,in}},\ p \rightarrow 0)$$

3. RESULTS AND DISCUSSION

3.1 Influence of the heat source inlet temperature

3.1.1 SIC optimization

Figure 1 shows that increasing the hot source inlet temperature leads to lower SICs. For the case when $\dot{m}_{\mathrm{hot}}$ = 10 kg/s and a T_{sink} = 15 °C, variations from 250 °C down to 120 °C cause an increase of more than 2450 $/kW for ammonia, more than 2000 $/kW for R32 and more than 2500 $/kW for R152a. The reason is that there is a higher amount of thermal energy available for the cycle when the inlet temperature of the heat source increases, which results into a higher cycle power output. The increased power output more than compensates the higher investment cost related to the larger heat transfer area of the primary heat exchanger.
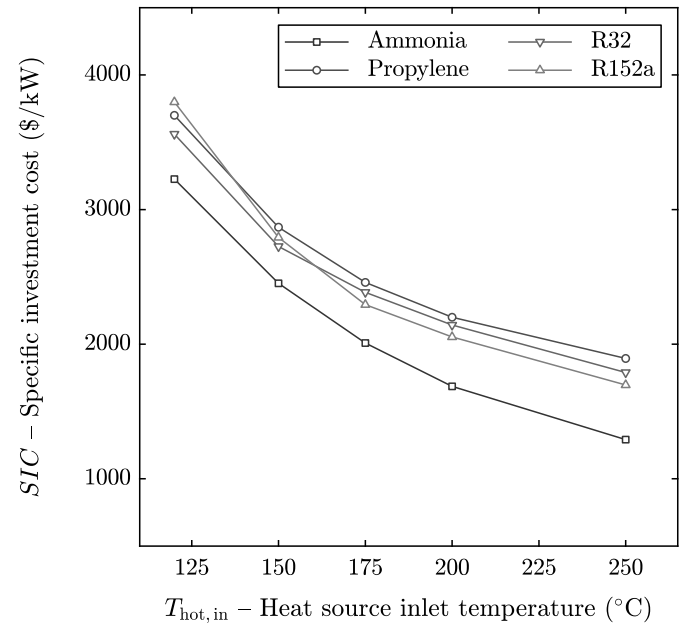
Figure 1: ORC optimum SIC evolution with $T_{\mathrm{h,\,in}}$

3.1.2 Second law efficiency optimization

As shown in *Figure 2*, the second law efficiency of the plant increases with the heat source inlet temperature up to a point where it reaches a maximum. Then, it starts to drop as the heat source inlet temperature further increases. The best thermodynamic performance of the plant corresponds to the point in which the constraint for maximum turbine inlet pressure becomes active. Beyond this point, the evaporating pressure cannot increase any further and the exergy destruction in the primary heat exchanger increases, leading to lower second law efficiencies. The only exception for this tendency is ammonia, for which the maximum turbine inlet temperature constraint remains inactive in the range of the studied conditions thanks to its higher critical temperature. Results shown in *Figure 2* indicate that there exists a working fluid that maximizes the efficiency of the plant for each temperature range. For instance, among the studied fluids, the best performance for the range $125\,°C \leq T_{hot,in} \leq 175°C$ was obtained for R32, for $175°C \leq T_{hot,in} \leq 200°C$, for R152a and, for a $T_{hot,in}$ higher than $200°C$, for ammonia. This indicates that working fluids with high critical temperatures are recommended for medium-to-high temperature heat sources, while, for low-temperature heat sources, working fluids with a low critical temperature are more suitable if the second law efficiency of the ORC wants to be maximized.
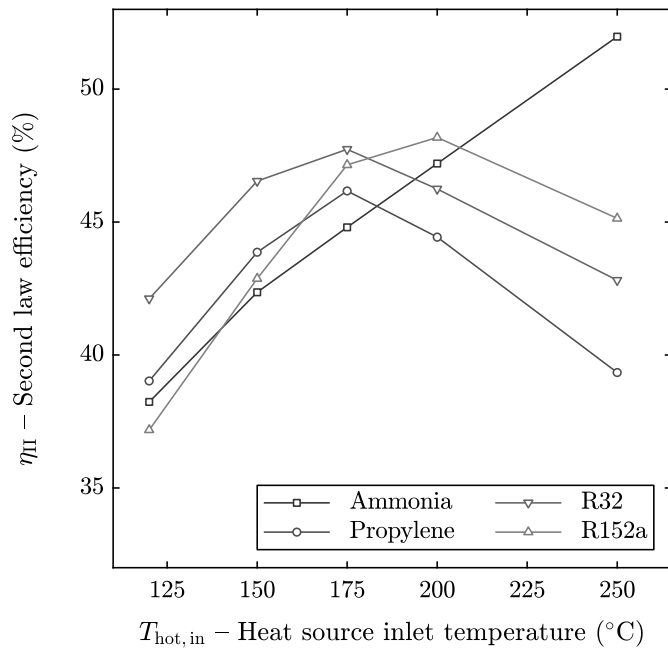
Figure 2: ORC optimum second law efficiency evolution with $T_{h,in}$

3.1.3 Optimization comparison

When comparing both optimizations, the efficiency of the cycle is lower when the SIC is minimized, and the cost is higher when the efficiency is maximized. This means that it is necessary to increase the cost of the system in order to increase the power output of an ORC power plant, and that this extra cost will vary depending on the working fluid. For example, improving the second law efficiency of R32 a 1% would require an extra SIC of 183 $/kW, while it would reach values up to 413 $/kW for R152a. These differences are a consequence of the different transport properties that each working fluid presents, which have an impact on the required heat transfer area and, therefore, on the cost of the plant.

The choice of objective function also affects the optimal cycle configuration in terms of evaporating and condensing temperatures and the degree of superheating (see the $T - s$ diagram of R152a in *Figure 3*). The evaporating pressure (and hence, the evaporating temperature) is always higher when optimizing the SIC of the ORC (32.5 bar vs. 28.5 bar, respectively). Increasing the evaporating pressure improves the heat transfer coefficients, leading to smaller heat transfer areas and higher power outputs, which both result into lower SICs. On the other side, the thermodynamic optimization does not take into consideration the cost of the plant and, for this reason, the evaporating pressure is set to a point at which the pinch point temperature can be minimized, leading to the lowest exergy destruction in the primary heat exchanger, which leads to the highest cycle efficiency.

Regarding the condensing pressure, this variable is always lower when optimizing the performance of the plant (7.5 bar vs. 5.5 bar). The reason is that the thermodynamic optimization tends to the lowest possible condensing pressure, in an effort to increase the power output and to reduce the LMTD to minimums (minimum exergy destruction), even though the cost of the plant considerably increases. On the other side, the SIC optimization tends to higher condensing pressures, which allow for smaller heat transfer areas because of the higher pinch points that are reached in the heat exchanger. This tendency has the disadvantage of reducing the pressure drop across the expander, reducing the cycle power output. Therefore, the SIC optimization tends to condensing pressure values that gives the best balance between smaller condensing area and higher power output.
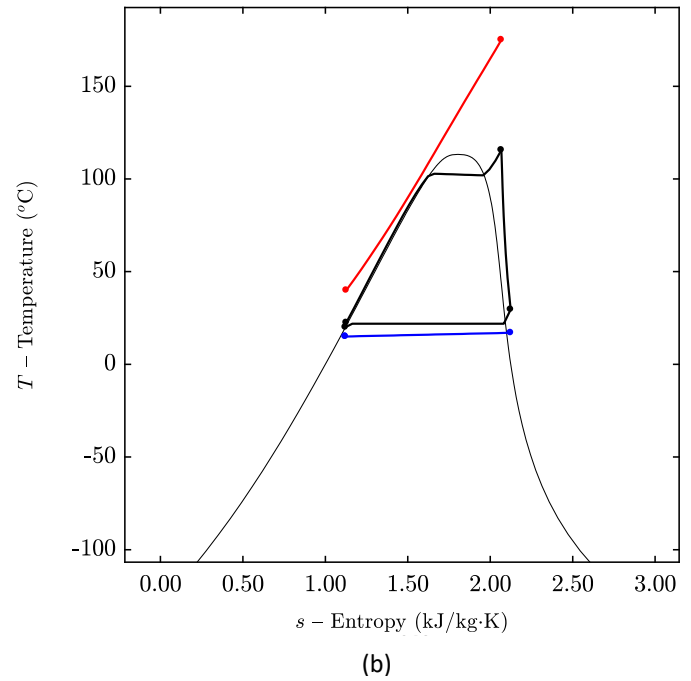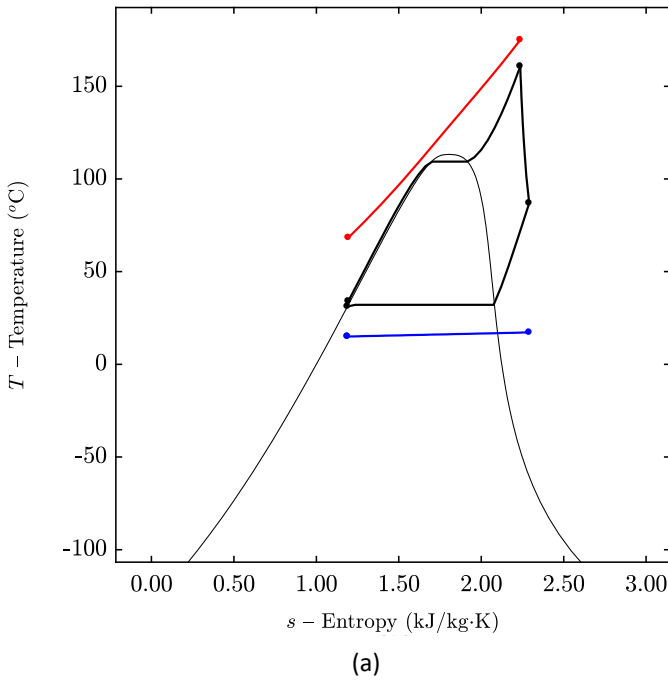
Figure 3: T-s diagrams for the SIC optimization (a) and the thermodynamic optimization (b) of R152a

Finally, there is an optimal non-zero degree of superheating when optimizing the SIC, and this effect was observed for all working fluids. Even though high degrees of superheating imply larger PrHE areas, its effect on the SIC is counteracted by a higher power output. Regarding the degree of superheating that results from the thermodynamic optimization, *Figure 3* shows that it is lower than the one obtained for the economic optimization, although this was not observed in all cases. Unlike with the degree of superheating when optimizing the SIC of the plant, there is not a clear tendency for the degree of superheating when optimizing the efficiency of the plant; it reaches high values under some scenarios, and very low ones under some others. This means that one may not determine a-priori the degree of superheating of the working fluid that maximizes the second law efficiency of the plant.

3.2 Influence of the heat source mass flow rate

The previously analyzed results were obtained for a hot source mass flow of 10 kg/s, for which the maximum net power output was lower than 1500 kW. In order to study larger capacity power plants, three different mass flow rates have been considered: 10 kg/s, 25 kg/s and 50 kg/s. *Table 2* shows the results for propylene, when $T_{c, in}$ = 15 °C and $T_{h, in}$ = 175 °C. As can be seen, increasing the hot source mass flow leads to higher investment costs, due to the greater size that all cycle components require. However, the greater power outputs that can be achieved thanks to the greater heat

inputs, are able to counteract the effect of increasing costs, resulting in lower SICs. This tendency was observed for all working fluids and for all $T_{c, in}$ and $T_{h, in}$ scenarios. This should be taken into consideration when designing high-flexibility ORC power plants, which are expected to operate at varying loads.

Table 2: Propylene's SIC optimization results for different hot source mass flows

$\dot{m}_{hot}$ [kg/s]	SIC [$/kW]	Cycle cost [M$]	$\dot{W}_{net}$ [kW]
10	2831	1.41	497
25	1943	2.23	1167
50	1497	3.30	2204

4. CONCLUSIONS

The following conclusions can be gathered from the results presented in this work:
1. Improving the thermodynamic performance of ORCs requires larger investment costs that result into higher SICs.
2. Higher hot source inlet temperatures and mass flows always lead to lower SICs, for all studied working fluids, in agreement with Quoilin et al. [2] and Imran et al. [4]. From the obtained results, the use of ammonia leads to the lowest SIC.
3. For each hot source inlet temperature range, there is a thermodynamic optimum working fluid that maximizes the power output, and hence the second law efficiency, of the cycle.

5

4. High evaporating and condensing pressures are desirable when minimizing the SIC of ORCs, while the contrary is preferable for optimizing the thermodynamic performance of the plant.

5. Small-capacity ORCs present higher SICs than large-capacity ORCs, even though the required initial investment is much higher for the second ones, being consistent with Lemmens [14].

REFERENCES

[1] E. Macchi, M. Astolfi, L. Bronicki, L. Bell, E. Lemmon, C. Ivernizzi, D. Bonalumi and F. Casella..., Organic Rankine Cycle (ORC) Power Systems. Technologies and Applications., E. M. a. M. Astolfi., Ed., Elsevier, 2017.

[2] S. Quoilin, S. Declaye, B. Tchanche and V. Lemort, "Thermo-economic optimization of waste heat recovery Organic Rankine Cycles," *Applied Thermal Engineering,* vol. 31, pp. 2885-2893, 17 May 2011.

[3] V. Le, A. Kheiri, M. Feidt and S. Pelloux-Prayer, "Thermodynamic and economic optimizations of waste heat to power plant driven by a subcritical ORC (Organic Rankine Cycle) using pure or zeotropic working fluid," *Energy,* vol. 78, pp. 622-638, 10 November 2014.

[4] M. Imran, M. Usman, B.-S. Park and Y. Yang, "Comparative assessment of Organic Rankine Cycle integration for low temperature geothermal heat source applications," *Energy,* vol. 102, pp. 473-490, 14 March 2016.

[5] N. Kazemi and F. Samadi, "Thermodynamic, economic and thermo-economic optimization of a new proposed organic Rankine cycle for energy production from geothermal resources," *Energy Conversion and Management,* vol. 121, pp. 391-401, 26 May 2016.

[6] R. Shah and D. Sekulic, in *Fundamentals of Heat Enchanger Design*, Kentucky, John Wiley & Sons, 2003, pp. 1-74.

[7] I. Encabo, R. Agromayor and L. Nord, "Techno-economic and thermodynamic optimiation of Rankine cycles. Master Thesis.," Trondheim, Norwegian University of Science and Technology, June,2018, pp. 37-49.

[8] R. Turton, R. Bailie, W. Whiting and J. Shaeiwitz, Analysis, Synthesis and Design of Chemical Processes, 3rd ed., Pearson Education, Inc, 2009.

[9] C. Zhang, C. Liu, S. Wang, X. Xy and Q. Li, "Thermo-economic comparison of subcritical organic Rankine cycle based on different heat exchanger configurations," *Energy,* no. 123, pp. 728-741, 2017.

[10] M. Astolfi, M. Romano, P. Bombarda and E. Macchi, "Binary ORC (Organic Rankine Cycles) power plants for the expliitation of medium-low temperature geothermal sources - Part B: Techno-economic optimization.," *Energy,* vol. 66, pp. 435-446, January 2014.

[11] Y. Li, M. Du, C. Wu, S. Wu and C. Liu, "Economical evaluation and optimization of subcritical organic Rankine cycle based on temperature matching analysis," *Energy,* no. 68, pp. 238-247, 2014.

[12] R. Agromayor and L. Nord, "Fluid selection and thermodynamic optimization of organic Rankine cycles for waste heat recovery applications," *Energy Procedia,* vol. 129, pp. 527-534, 2017.

[13] I. E. Cáceres, R. Agromayor and L. O. Nord, "Thermodynamic Optimization of an Organic Rankine Cycle for Power Generation from a Low Temperature Geothermal Heat Source.," in *Proceedings of the 58th SIMS.*, Reykjavik, 2017.

[14] S. Lemmens, "Cost Engineering Techniques and Their Applicability for Cost Estimation of Organic Rankine Cycle Systems," *Energies,* vol. 9, no. 485, p. 18, 2016.